THE JOURNAL OF BIOLOGICAL CHEMISTRY
Vol. 275, No. 5, Issue of February 4, pp. 3645–3654, 2000

Printed in U.S.A.

The Amyloid Precursor-like Protein 2 Associates with the Major Histocompatibility Complex Class I Molecule K^d*

(Received for publication, October 15, 1999)

Martina Sester‡, Dominik Feuerbach§, Rainer Frank¶, Tobias Preckel‖, Anja Gutermann, and Hans-Gerhard Burgert**

From the Max von Pettenkofer-Institut, Department of Virology, Genzentrum, Feodor-Lynen-Str. 25, 81377 München, Germany and ¶Center for Molecular Biology Heidelberg, 69120 Heidelberg, Germany

Amyloid precursor-like protein 2 (APLP2) is a member of a protein family related to the amyloid precursor protein, which is implicated in Alzheimer's disease. Little is known about the physiological function of this protein family. The adenovirus E3/19K protein binds to major histocompatibility complex (MHC) class I antigens in the endoplasmic reticulum, thereby preventing their transport to the cell surface. In cells coexpressing E3/19K and the MHC K^d molecule, K^d is associated with E3/19K and two cellular protein species with masses of 100 and 110 kDa, termed p100/110. Interestingly, p100/110 are released from the complex upon the addition of K^d-binding peptides, suggesting a role for these proteins in peptide transfer to MHC molecules. Here we demonstrate by microsequencing, reactivity with APLP2-specific antibodies, and comparison of biochemical parameters that p100/110 is identical to human APLP2. We further show that the APLP2/K^d association does not require the physical presence of E3/19K. Thus, APLP2 exhibits an intrinsic affinity for the MHC K^d molecule. Similar to the binding of MHC molecules to the transporter associated with antigen processing, complex formation between APLP2 and K^d strictly depends upon the presence of β_2-microglobulin. Conditions that prolong the residency of K^d in the endoplasmic reticulum lead to a profound increase of the association and a drastic reduction of APLP2 transport. Therefore, this unexpected interplay between these unrelated molecules may have implications for both MHC antigen and APLP2 function.

The predominant proteinaceous constituent of senile plaques observed in Alzheimer's disease is the amyloid peptide derived from amyloid precursor protein (APP)[1] (1). APP belongs to a larger gene family that includes the mammalian amyloid precursor like proteins 1 and 2 (APLP1 and -2) (2–5) as well as the *Drosophila* protein APPL (6) and the *Caenorhabditis elegans* protein APL-1 (7). Despite advances in understanding the biochemical and molecular properties and the regulation of the members of this gene family, their physiological function is not understood (1). APP knockout mice exhibit a weak phenotype with retarded neurite outgrowth (8), while APLP2 knockout mice appear phenotypically normal (9) or die at an early embryonic stage (10).

APLP2 is ubiquitously expressed. Alternative splicing of APLP2 pre-mRNA generates at least four transcripts, two of which encode a Kunitz protease inhibitor domain (KPI) (3, 11). Many structural features of APLP2 are reminiscent of a cell surface receptor. It is a large type I transmembrane protein whose sequence predicts a number of distinct domains; an N-terminal cysteine-rich domain exhibiting zinc, copper, and heparin binding activity (12) is followed by a very acidic region and, depending on the isoform, the KPI domain. All of these domains have their respective counterparts in APP. A very high degree of similarity between APLP2 and APP is found in the region following the KPI domain while the similarity decreases drastically in the ~100 amino acids (aa) preceding the transmembrane and cytoplasmic domains, which again exhibit a high sequence identity (3, 4, 13). Biosynthesis and trafficking seems to follow initially the constitutive secretory pathway; upon synthesis and translocation into the ER, *N*-linked carbohydrates are added. Transport through the Golgi apparatus results in *O*-glycosylation and, depending on the splice variant, the addition of a chondroitin sulfate glycosaminoglycan (14, 15). The ectodomain can be cleaved in a post-Golgi compartment or at the plasma membrane and is then secreted (15, 16).

A similar pathway is followed by major histocompatibility complex (MHC) class I molecules, which bind peptides in the ER for presentation on the cell surface to cytotoxic T cells (17). Completely assembled MHC I molecules consist of three subunits: an MHC encoded polymorphic transmembrane glycoprotein (heavy chain; HC) with an apparent molecular mass of ~45 kDa is noncovalently associated with a soluble light chain of 12 kDa, called β_2-microglobulin (β_2m), and an 8–10-aa-long peptide. Assembly of MHC I molecules occurs in the ER and is assisted by a number of chaperones (18–20). Initially, the free HC associates with the ER-resident chaperone calnexin, an integral membrane protein of ~90 kDa. In human cells, binding of β_2m to the HC triggers the dissociation from calnexin. The labile HC/β_2m heterodimer is stabilized and further folded by other chaperones of the ER quality control machinery, such as calreticulin and ERp57, before being loaded with peptides (21–23). The bulk of MHC I antigen-bound peptides arise from

* This work was supported by Deutsche Forschungsgemeinschaft Grants SFB 388 and Bu 642/1 (to H.-G. B.). The costs of publication of this article were defrayed in part by the payment of page charges. This article must therefore be hereby marked "*advertisement*" in accordance with 18 U.S.C. Section 1734 solely to indicate this fact.

‡ Present address: University of Homburg, Med. Dep. IV, 66421 Homburg, Germany.

§ Present address: Novartis, Preclinical Research 386.725, CH-4002 Basel, Switzerland.

‖ Present address: Hewlett Packard GmbH, Waldbronn, Analytical Division, Hewlett Packard Strasse 8, 76337 Waldbronn, Germany.

** To whom correspondence should be addressed. Tel.: 49-2180-6852; Fax: 49-2180-6899; E-mail: burgert@lmb.uni-muenchen.de.

[1] The abbreviations used are: APP, amyloid precursor protein; Ad, adenovirus; APLP1 and -2, amyloid precursor-like protein 1 and 2, respectively; β_2m, β_2-microglobulin; BFA, brefeldin A; GAG, glycosaminoglycan; CS-GAG, chondroitin sulfate glycosaminoglycan; E3, early region 3; ER, endoplasmic reticulum; HC, heavy chain; KPI, Kunitz type of protease inhibitor; mAb, monoclonal antibody; MHC, major histocompatibility complex; PAGE, polyacrylamide gel electrophoresis; TAP, transporter associated with antigen processing; aa, amino acid(s).

protein degradation within the cytosol. A specialized transporter associated with antigen processing (TAP) translocates these peptides into the ER (18, 20, 24). In general, loading of MHC molecules with optimal peptides requires a physical association with TAP, which is mediated by tapasin, a 48-kDa protein encoded in the MHC (25, 26). However, most of the accessory proteins are not absolutely essential for efficient cell surface expression of MHC I molecules, and different alleles differ in their requirement to interact with tapasin and TAP (27, 28). Upon loading with peptide, class I heterotrimers dissociate from TAP and are efficiently exported to the cell surface (18). Additional molecules like gp96 (29), p100/110 (30), p100 (31), or p62 may participate in the assembly process of MHC I molecules with peptides (22, 32). However, their precise role and their temporal order of action are poorly defined.

Subversion of the MHC I assembly and antigen presentation pathway seems to be a common strategy employed by persistent viruses to escape immunosurveillance by their host (reviewed in Refs. 33–35). For example, the human adenovirus (Ad) early region 3 (E3) glycoprotein E3/19K binds to MHC I molecules in the ER and inhibits transport of MHC I molecules to the cell surface (36, 37). Consequently, MHC-restricted cytotoxic T cell lysis is severely suppressed (Refs. 33, 38, and 39 and references therein).

The function of the E3/19K protein is based on two activities; an HLA binding activity is combined with the ability to localize to the ER. This latter feature appears to require an ER retrieval motif in the cytoplasmic tail (40–42) consisting of two lysines, KK*XX* or K*X*K*XX*, positioned either in −3 and −4 or −3 and −5 from the carboxyl terminus. Proteins containing these dilysine motifs can reach the *cis*-Golgi, where they are bound by specific cytosolic coat proteins that mediate retrograde transport to the ER (43, 44).

Complex formation between MHC molecules and E3/19K is primarily mediated by their luminal domains (33, 45–48). Binding of MHC molecules to E3/19K is determined by their polymorphic α1 and α2 domains comprising the peptide binding pocket (46, 48), while the HLA binding capacity of the Ad2 E3/19K protein is critically dependent on two intramolecular disulfide bonds within its luminal domain (47, 49). At exactly which stage of the MHC assembly E3/19K associates with MHC molecules is unknown.

In cells expressing the murine MHC K^d allele and E3/19K, the K^d-E3/19K complex is associated with two additional cellular transmembrane proteins of 100 and 110 kDa, termed p100/110. Interestingly, K^d-binding peptides can displace p100/110 from the MHC-E3/19K complex, suggesting a role of these proteins in peptide transfer to MHC I molecules (30).

We have now identified p100/110 as the APLP2 protein. Microsequencing of purified p100/110 revealed peptide sequences identical to APLP2, and antibodies raised against APLP2 recognize proteins with identical biochemical properties to p100/110. Furthermore, we show that APLP2 exhibits an intrinsic affinity for murine MHC K^d molecules that is markedly increased in the presence of the Ad2 E3/19K molecule. E3/19K promotes complex formation between APLP2 and K^d by retaining K^d in the ER. In doing so, the viral protein also impairs trafficking of APLP2. The potential implications of this unexpected finding for both MHC I and APLP2 function are discussed.

EXPERIMENTAL PROCEDURES

Plasmids, Cell Lines, Culture Conditions, and Transfections—Transfection of 293 cells (ATCC CRL 1573) with the Ad2 *Eco*RI-D and *Eco*RV-C fragment led to the establishment of 293.12 and 293E3–45 cell lines, respectively, constitutively expressing E3/19K (36, 50). 293K^d2 and 293.12K^d8 were generated by transfection of 293 and 293.12 cells, respectively, with the murine H-2K^d gene (38). The murine embryonic fibroblast cell line B7 was established from BALB/c mice by transformation with SV40 (51) and was kindly provided by H. Hengel (Max von Pettenkofer-Institut Munich, Germany). B7E3–28 cells were derived from B7 by transfection with the Ad2 *Eco*RV-C fragment. The human melanoma cell line FO-1 (kindly provided by S. Ferrone, Medical College of New York) does not express β_2m (52). For generating FO-1K^d and FO-1$K^d\beta$ cells, FO-1 cells were transfected with the K^d gene and both the K^d and human β_2m genes, respectively. Clones were selected upon cotransfection of the neomycin resistance gene and subsequent culture in medium containing 800 μg/ml G418 (Life Technologies, Inc., Eggenstein, Germany). Cell line 293APP was generated by transfection of 293 cells with the expression vector hAPP770CMV5, a kind gift of K. Beyreuther (ZMBH, University of Heidelberg, Germany). This plasmid contains the coding region for human APP770 under the control of the cytomegalovirus early promoter (53). The K^dE3 construct encodes a chimeric molecule comprising the luminal and transmembrane part of H-2K^d fused to the cytoplasmic tail of Ad2 E3/19K. The cDNA (54), kindly provided by J. R. Bennink (National Institutes of Health, Bethesda, MD), was subcloned into the expression vector pCMV5 (55) using restriction enzymes *Sal*I and *Sma*I.

All cells were grown in Dulbecco's modified Eagle's medium containing 10% fetal calf serum, 2 mM glutamine, and antibiotics. For routine culture of 293 transfectants, the medium was supplemented with 200 μg/ml G418. Medium for double transfectants of 293 cells contained in addition 100 μg/ml hygromycin (Calbiochem).

Monoclonal Antibodies (mAbs) and Antisera—The following monoclonal antibodies were used in this study: W6/32 (ATCC HB95; anti-HLA-A, -B, and -C; Tw1.3, anti-E3/19K (42); 34-1-2 (ATCC HB79) (directed to the α1/α2 domain of H-2K^d, D^d); and SF1–1.1.1 (ATCC HB 159) reacting with the α3 domain of H-2K^d. Polyclonal rabbit antisera AP tail and Kc were generated by immunization with the peptides CYENPTYKYLEQMQI and CKVMVHDPHSLA, corresponding to the C terminus of APLP2 and K^d, respectively. Peptides CTKIIGSVSKEEEEE and CADMDQFTASISET, representing amino acids 206–219 and 570–582 of APLP2, respectively, were used to raise antisera AP 206 and AP 570. The N-terminal cysteine was added for directed coupling to keyhole limpet hemocyanin or bovine serum albumin. Coupling and immunization was done essentially as described (47). The polyclonal antibody APP tail raised against the 20 C-terminal amino acids of human APP (56) was a kind gift of V. Herzog (University of Bonn, Germany).

Purification of p100/110—The source for large scale purification of p100/110 was 293.12K^d8 cells, which were grown on 510-cm^2 dishes, trypsinized, and centrifuged at 300 × *g*. The pellet was frozen in liquid nitrogen and stored at −70 °C until use. Approximately 9×10^9 cells were used for purification. The protocol below is outlined for 2×10^9 cells. Cells were lysed in 100 ml of lysis buffer (1% Nonidet P-40, 100 mM NaCl, 5 mM $MgCl_2$, 20 mM Tris, pH 7.4). The cleared lysate was incubated with 1 mg of mAb 34-1-2 bound to 1 ml of protein A-Sepharose (Amersham Pharmacia Biotech, Uppsala, Sweden) for 3 h. Thereafter, the protein A pellet was washed three times with washing buffer B (0.2% Nonidet P-40, 10 mM Tris, pH 7.6, 0.15 M NaCl, 2 mM EDTA, pH 8.0), twice with buffer C (0.2% Nonidet P-40; 10 mM Tris, pH 7.6; 0.5 M NaCl; 2 mM EDTA, pH 8.0), and once with 10 mM Tris, pH 8.0. Bound antigens were eluted two times with 1.5 ml of 10 mM octyl glucoside, 0.2 M sodium acetate, pH 2.7. The supernatants were immediately neutralized, combined, and incubated with protein A beads for 1 h to adsorb most of the antibodies. Upon centrifugation, the supernatant was concentrated using a Centricon 100 device (Amicon). After the addition of 2 ml of 10 mM octyl glucoside, 5 mM Tris, pH 8.0, the material was concentrated again and stored at −70 °C. Proteins contained in the eluate, including p100/110, antibody, E3/19K, K^d, and β_2m, were separated by SDS-polyacrylamide gel electrophoresis (SDS-PAGE). The gel was briefly stained with Coomassie Brilliant Blue and washed several times in water. The two bands, approximately 15 μg each, were precisely excised, and gel slices were cut in pieces (about 1 × 1 mm^2) and incubated for 16 h in water with frequent changes. The washed gel pieces were then immersed in 200 μl of 100 mM ammonium hydrogen carbonate (pH 8.5) containing trypsin at an enzyme/protein mass ratio of approximately 1:5. Following incubation at 37 °C for 8 h, the protein fragments produced were eluted from the gel by shaking the pieces twice for 3 h in an equal volume of 0.1% trifluoroacetic acid in water. Residual water was extracted from the gel matrix by treatment with acetonitrile. The concentrated eluates were extracted twice with isoamyl alcohol/heptane (1:4) to remove traces of SDS. Separation of the tryptic peptides was performed by reversed-phase high performance liquid chromatography on a Vydac 218TP5 column (1.6 × 250 mm). Two peaks were selected from each elution diagram, and the material was

subjected to gas phase sequence analysis.

Metabolic Labeling, Preparation of Microsomes, Tunicamycin Treatment, Brefeldin A Treatment, Immunoprecipitation, and SDS-PAGE—Labeling of cells with [^{35}S]methionine (Amersham Pharmacia Biotech, Braunschweig, Germany), tunicamycin treatment, immunoprecipitation, and SDS-PAGE were done essentially as described (36, 46). Quantitative analysis of immunoprecipitates was carried out using a phosphor imager (Fujix Bas 1000; Fuji, Japan). Microsomes were prepared as described previously (30).

For sequential immunoprecipitation, the lysate was incubated for 30 min with the first antibody. Protein A-Sepharose was added, and the incubation continued for 45 min. This first immunoprecipitation was repeated, and the lysate was cleared from residual antibody by two sequential incubations with protein A-Sepharose for 45 min. Subsequently, a second specific antibody was added, and immunoprecipitation was performed as described before.

Brefeldin A (BFA) treatment was initiated 3 h before starvation of cells by replacing the medium with medium supplemented with 2.5 μg/ml brefeldin A (Sigma, Deisenhofen, Germany). This concentration was kept throughout the starving and labeling period.

Endoglycosidase F Treatment—Endoglycosidase F treatment was carried out as described (30) except that 8 μg/ml phenylmethylsulfonyl fluoride (Sigma) was included during the incubation.

Western Blotting—Immunoblotting was carried out as described (47, 57).

RESULTS

Peptide Sequences from Purified p100/110 Are Identical to APLP2—Immunoprecipitation of the MHC K^d molecule from cells expressing the adenovirus protein E3/19K reveals not only MHC class I heavy chain (K^d), E3/19K, and β_2m but also two additional protein species with apparent molecular masses of ~100 and 110 kDa, termed p100/110 (Fig. 1*A*, *lane 1*; Ref. 30). To elucidate the molecular nature of p100/110 by microsequencing, these proteins were large scale purified from 293.12K^{d}8 cells, constitutively expressing both K^d and E3/19K upon transfection of 293 cells (38). Detergent extracts of approximately 9×10^9 293.12K^{d}8 cells were incubated with mAb 34-1-2 directed to MHC K^d molecules. Immunoprecipitated material containing coimmunoprecipitated p100/110 was eluted from the protein A-beads by low pH treatment, concentrated, and separated by preparative SDS-PAGE. Fig. 1*A* (*lanes 2* and *3*) shows the typical protein pattern obtained following this purification scheme. Apart from p100/110, K^d HC, and E3/19K, Coomassie staining reveals two prominent bands above the K^d HC and E3/19K, corresponding to the heavy and light chain of the mAb, respectively (Fig. 1*A*, compare *lanes 2* and *3* with *lane 4).* Additional protein bands below the p100/110 bands are also detected. Bands corresponding to p100 and p110, respectively, were excised from a Coomassie Blue-stained gel and separately digested with trypsin. Fragments were separated by reversed-phase high performance liquid chromatography, and from each digest two prominent peptide peaks were analyzed by microsequencing. Data base searches revealed a 100% identity of all four peptides to the human APLP2. Fig. 1*B* shows the putative amino acid sequence of the APLP2 protein (3–5). Peptides sequenced from p100 and p110 are *boxed*. Peptide 4 was derived from p100, peptide 3 was derived from p110, and peptide 1/2 was obtained twice, once from p100 and once from the p110 digest.

Antibodies Directed to APLP2 Recognize Proteins with the Same Apparent Molecular Mass as That of p100/110—Since the p100/110 preparation still contained minor contaminants, we could not exclude the possibility that these are the source of the sequenced peptides. Therefore, we tried to obtain independent evidence for the identity of APLP2 with p100/110. Polyclonal antisera were raised against three different peptides of human APLP2 (Fig. 1*B*, *thick underline*). Antiserum AP tail is directed to the 14 C-terminal amino acids of the APLP2 cytoplasmic tail. This peptide was chosen, since antibodies against

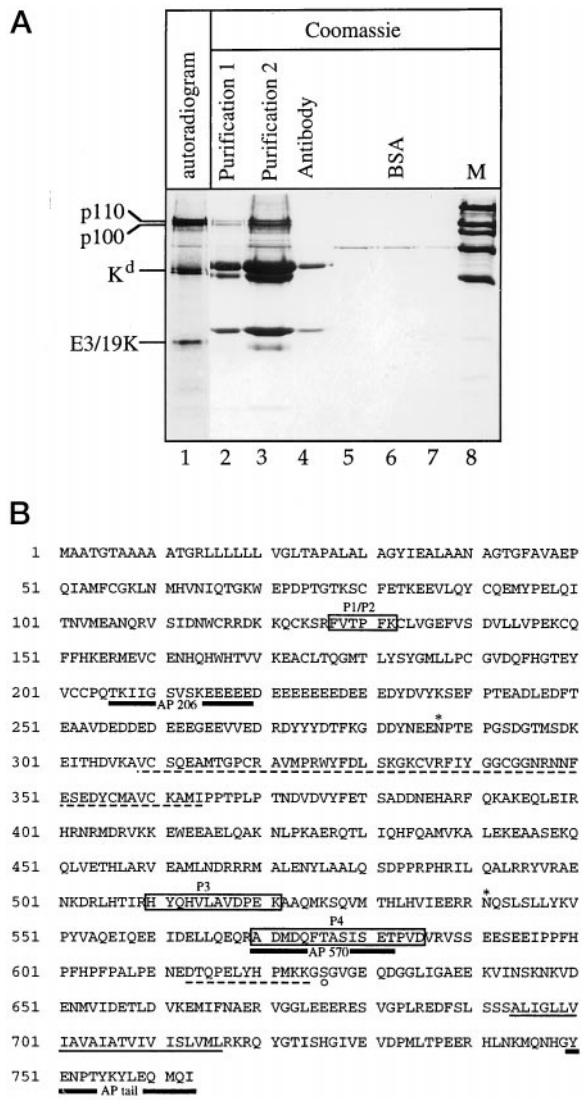

FIG. 1. **Purification of p100/110 by coimmunoprecipitation with the MHC K^d molecule.** *A*, a total of 9×10^9 293.12K^{d}8 cells were lysed in Nonidet P-40-containing buffer, and K^d was immunoprecipitated with mAb 34-1-2. After elution and concentration of the protein A-bound material, a fraction representing material derived from approximately 2×10^8 (*lane* 2) and 5×10^8 (*lane* 3) cells was loaded on an 8% polyacrylamide minigel. As control, 5 μg of purified mAb 34-1-2 (*lane* 4) and for quantitative evaluation 400 ng (*lane* 5), 300 ng (*lane* 6), and 200 ng (*lane* 7) of bovine serum albumin (*BSA*) were loaded. Identification of the Coomassie-stained proteins was possible by comparison with the migration position of immunoprecipitated proteins from metabolically labeled (4 h) cells (*lane* 1). *B*, amino acid sequence of human APLP2. Peptides microsequenced from purified p100/110 are *boxed*. Peptides 1 and 2 were obtained from both p100 and p110. Peptide 3 was sequenced from p110 and peptide 4 from p100. The predicted transmembrane region is *underlined*. Potential *N*-glycosylation sites and the site for glycosaminoglycan addition are indicated by an *asterisk* and an *open circle*, respectively. *Stippled lines* indicate alternatively spliced regions. The peptides used to raise rabbit antisera AP 206, AP 570 and AP tail have a *thick underline*.

cytoplasmic portions of proteins are likely to react with the native protein. Antiserum AP 570 recognizes a peptide overlapping with P4 that was sequenced from p100 (Fig. 1*B*). Since murine and human APLP2 display an identity of 92.9% at the amino acid level, the animals used for immunization might be tolerant to these peptides. Therefore, a third peptide encompassing amino acids 206–219 that is poorly conserved between mouse and human APLP2 (only 6 of 14 aa are identical) was selected to raise antiserum AP 206. All three sera were tested for their ability to immunoprecipitate APLP2 from detergent

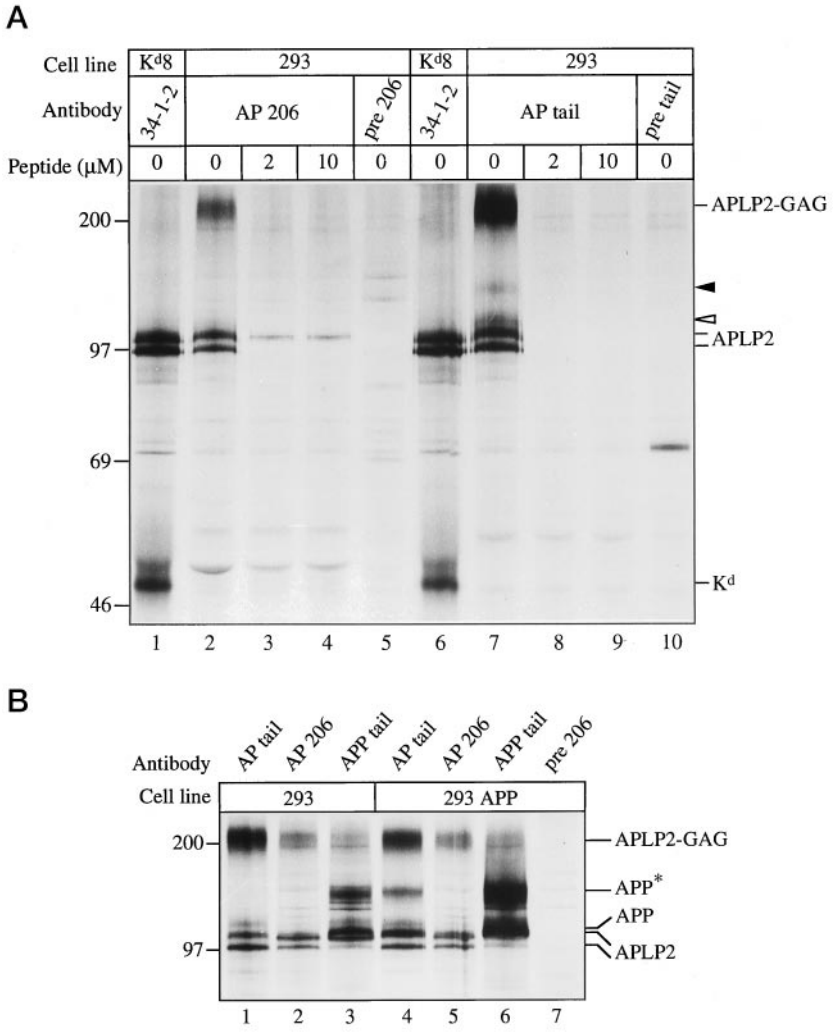

FIG. 2. **The polyclonal antibodies AP tail and AP 206 recognize APLP2 in detergent lysates.** *A*, 293 cells were labeled for 1 h with 100 μCi/ml [^{35}S]methionine and lysed with buffer containing 1% Nonidet P-40. APLP2 was immunoprecipitated with antisera AP tail (*lanes 7–9*) and AP 206 (*lanes 2–4*). Lysates immunoprecipitated in *lanes 3* and *4* and *lanes 8* and *9* contained 2 and 10 μM, respectively, of the peptide used for immunization. *Lanes 5* and *10* are control reactions with the respective preimmune sera (*pre*). Immunoprecipitates from 293.12K^{d}8 cells using mAb 34-1-2 show coprecipitating proteins p100/110 comigrating with APLP2 (*lanes 1* and *6*). The *numbers* on the *left* represent the migration of molecular mass marker proteins in kDa. The *open* and *closed arrowheads* mark presumed APP proteins. APLP2-GAG indicates the position of the glycosaminoglycan-modified form of APLP2. *B*, specificity of antibodies AP tail and AP 206. 293 cells (*lanes 1–3*) and 293 cells overexpressing APP770 (293APP; *lanes 4–7*) were labeled as described for Fig. 2*A*, and APLP2 and APP were immunoprecipitated with antisera AP tail, AP 206, APP tail, and preimmune serum (*pre 206*) as indicated at the *top*. The positions of the respective proteins are indicated. Please note that the APP tail serum, which recognizes two major forms of APP (APP and APP*) cross-reacts with APLP2 and APLP2-GAG.

lysates. Antiserum AP 570 did not recognize APLP2 in detergent lysates, but it detected proteins with the same apparent molecular mass as APLP2 after SDS denaturation and/or Western blotting (Fig. 3*C*; see below). This indicates that the corresponding peptide is not accessible within the native molecule. Therefore, for most experiments, AP 206 and AP tail were used. Using metabolically labeled 293 cell lysates, both sera specifically immunoprecipitate proteins with apparent molecular masses of ~100, 110, and 210–230 kDa (Fig. 2*A*, *lanes 2* and *7*). The specificity of the antisera was confirmed by showing that none of these proteins are precipitated with the respective preimmune sera (Fig. 2*A*, *lanes 5* and *10*) or upon the addition to the lysates of the respective peptides used for immunization (Fig. 2*A*, *lanes 3* and *4* and *lanes 8* and *9*). The more diffuse band with an apparent molecular mass of ~220 kDa appears to represent a glycosaminoglycan (GAG)-modified form of human APLP2, since its molecular mass is reduced by cleavage with chondroitinase ABC (data not shown). A similar modification was noted previously for murine APLP2 (15). We conclude that the peptide-specific antisera recognize APLP2.

Remarkably, the 100- and 110-kDa APLP2-specific protein species comigrate with p100/110 coprecipitated with K^d from detergent lysates of 293.12K^{d}8 cells using the K^d-specific antibody 34-1-2 (Fig. 2*A*, *lanes 1* and *6*). This indicates that both proteins are identical. However, the CS-GAG-modified form of APLP2 is not observed in 34-1-2 immunoprecipitates of 293.12K^{d}8 lysates and is hardly detectable using the rabbit antisera against APLP2 (see below).

The high degree of sequence similarity (71%) between human APLP2 and APP (11 of 14 amino acids of the AP tail peptide are identical), the appearance of two additional bands in the AP tail precipitate (*open* and *closed arrowheads* in Fig. 2*A*), and the recently noted cross-reactivity of many "APP-specific" antibodies with APLP2 (13) prompted us to test whether our sera also cross-reacted with APP. To increase the APP-specific signal in 293 cells and to better be able to distinguish between APLP2 and APP, we generated a cell line (293APP) stably overexpressing the largest APP isoform, APP770. 293 and 293APP cells were labeled with [^{35}S]methionine, and lysates were subjected to immunoprecipitation with antisera raised against APLP2- and APP-specific peptides (Fig. 2*B*). In 293APP cells, the APP serum recognizes two prominent proteins termed APP and APP*, which are also present in immunoprecipitates of AP tail but not in those of AP 206 (Fig. 2*B*, compare *lane 6* with *lanes 4* and *5*). Thus, the AP 206 serum is specific for APLP2, while the AP tail serum also recognizes APP. However, since the reactivity of AP 206 to APLP2 seemed to be significantly lower compared with that of AP tail (Fig. 2*B*, *lanes 1* and *2*, or Fig. 2*A*, *lanes 2* and *7*) and coprecipitation of endogenous APP with AP tail was only marginal using detergent extracts of untransfected 293 cells (Fig. 2*B*, *lane 1*), most subsequent experiments were performed with the AP tail serum.

To further substantiate our conclusion that APLP2 and p100/110 are identical, several biochemical properties of these molecules were compared. For example, the *N*-linked glycosy-

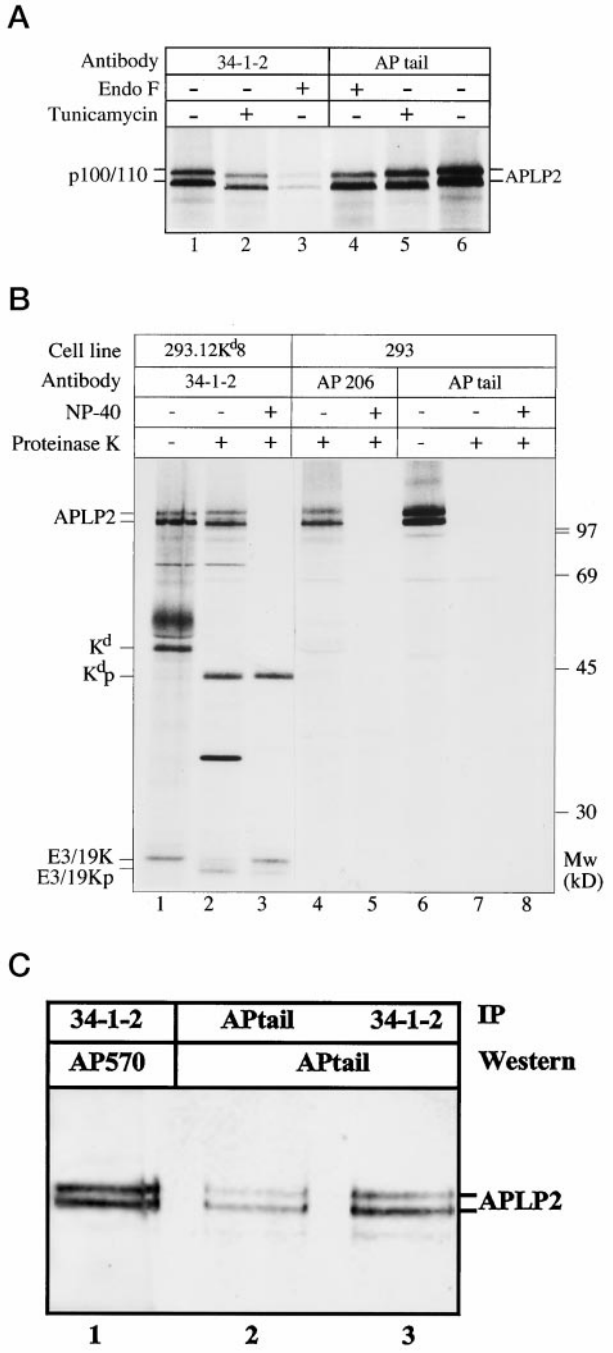

FIG. 3. **P100/110 and APLP2 share the same biochemical properties.** *A*, P100/110 and APLP2 exhibit the same pattern of *N*-glycosylation. After labeling of 293.12K^{d}8 cells, p100/110 and APLP2 were precipitated using mAb 34-1-2 (*lanes 1–3*) and AP tail (*lanes 4–6*), respectively. Cells were either treated with 7 μg/ml tunicamycin for 1 h prior to and during the labeling period (*lanes 2* and *5*), or proteins were treated with 0.5 units of endoglycosidase F (*Endo F*) after immunoprecipitation (*lanes 3* and *4*). As controls for the tunicamycin and endoglycosidase F treatment, cells and immunoprecipitates were mock-treated (*lanes 1* and *6*). *B*, P100/110 and APLP2 have the same transmembrane orientation. 3×10^7 293.12K^{d}8 cells (*lanes 1–3*) and 293 cells (*lanes 4–8*) were labeled for 35 min with 125 μCi/ml of [^{35}S]methionine. Microsomes were prepared and treated with proteinase K or Nonidet P-40 as indicated at the *top*. Immunoprecipitation was carried out with mAb 34-1-2, AP 206, and AP tail. The positions of APLP2, K^d, and E3/19K are marked. *p* denotes proteinase K-cleaved forms of the precipitated proteins. The *numbers* on the *right* represent molecular weight marker proteins in kDa. *C*, antibodies against APLP2 recognize p100/110 coprecipitated with K^d in Western blots. Lysates derived from 5×10^6 293.12K^{d}8 cells were incubated with AP tail (*lane 2*) or 34-1-2 (*lanes 1* and *3*). Immunoprecipitated (*IP*) material was separated by SDS-PAGE and transferred to a nylon membrane that was incubated with AP 570 (*lane 1*) and AP tail (*lanes 2* and *3*). Upon incubation with alkaline phosphatase-coupled antibodies against rabbit IgG, phosphatase activity was developed by NBT/BCIP.

lation of p100/110 and APLP2 was examined in two ways. First, 293.12K^{d}8 cells were labeled with [^{35}S]methionine in the absence (Fig. 3*A*, *lanes 1* and *6*) or presence (Fig. 3*A*, *lanes 2* and *5*) of tunicamycin, an inhibitor of *N*-glycosylation. Second, immunoprecipitates of metabolically labeled cells were treated with endoglycosidase F, an enzyme that removes *N*-linked carbohydrates except for one *N*-acetylglucosamine (Fig. 3, *lanes 3* and *4*). Both treatments reduced the molecular mass of p100/110 and APLP2 by ~3 kDa. Hence, *N*-glycosylation of p100/110 and APLP2 appears to be identical. A similar treatment of the K^d protein, known to bear three *N*-linked carbohydrates, reduces its molecular mass by ~7.5 kDa (data not shown). Thus, only one (N541) of the two potential glycosylation sites (NQS and NPT) of APLP2 appears to be used. This can be explained by the nonfavorable sequence context of asparagine 287 (N*X*T, where *X* represents proline; Fig. 1*B*), which may prevent its glycosylation (58).

APLP2 is supposed to be a type I integral membrane protein (3, 4, 13). Removing the putative cytoplasmic tail of the molecule should therefore reduce its apparent molecular mass by about 5.7 kDa. This was confirmed by incubating microsomes isolated from radiolabeled cells with or without proteinase K. APLP2 and p100/110 were immunoprecipitated using antibodies against APLP2 (AP tail and AP 206) and K^d (34-1-2), respectively (Fig. 3*B*). In line with the prediction made above, treatment with proteinase K abrogates recognition of APLP2 by the antiserum AP tail directed to the cytoplasmic tail of APLP2 (Fig. 3*B*, compare *lanes 6* and *7*). In contrast, antiserum AP 206 directed to the luminal part of APLP2 still precipitated the two protein species, which migrate slightly faster compared with that from nontreated microsomes (compare *lane 1* with *lane 4*). A similar size reduction is observed upon proteinase K treatment of p100/110 immunoprecipitated from 293.12K^{d}8 cells with mAb 34-1-2 (Fig. 3*B*, compare *lane 2* with *lane 4*). The specificity of the protease digestion is confirmed in that the known type I transmembrane proteins K^d and E3/19K are shortened to the length expected after removal of their cytoplasmic tail (K^{d}p and E3/19Kp), whereas the position of the luminal protein β_2m was unaltered (data not shown), indicating proper sealing of the microsomes. The 32-kDa band detected in immunoprecipitations of K^d after proteinase K treatment (Fig. 3*B*, *lane 2*) is not observed in APLP2 precipitations. Therefore, this fragment is obviously derived from other proteins coprecipitating with K^d molecules, most likely those appearing as a diffuse band with an apparent molecular mass of 50–55 kDa. Taken together, we conclude that p100/110 and APLP2 have the same transmembrane orientation.

More direct evidence for the identity of p100/110 with APLP2 was obtained by reprecipitation (data not shown) and Western blotting of K^d-associated material with APLP2-specific antisera. All three APLP2-specific sera recognized p100/110 coprecipitated by the K^d-specific antibody 34-1-2 in Western blots (Fig. 3*C* and data not shown). Moreover, V8 protease digestion of the lower and higher molecular forms of APLP2 results in peptide maps identical to those of p100 and p110, respectively (data not shown). Like p100 and p110, the APLP2 maps differ in the lower molecular weight range, confirming our previous interpretation that p100 and p110 and thus the two forms of APLP2 are derived from the same protein by differential splicing (30). Therefore, by all criteria tested (peptide sequencing, recognition by APLP2-specific antisera, biochemical properties, and V8 maps), p100/110 is identical to APLP2.

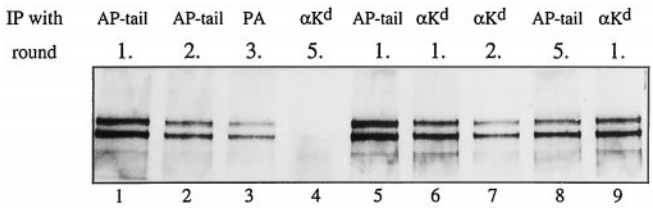

FIG. 4. **A large fraction of APLP2 is associated with K^d.** APLP2 was sequentially immunoprecipitated from metabolically labeled 293.12K^d8 cell lysates. After two rounds of immunoprecipitation with AP tail (*lanes 1* and *2*), the lysate was cleared two times with protein A-Sepharose from residual antibody (*lane 3*; first round of protein A-Sepharose) and subjected to immunoprecipitation (*IP*) with mAb 34-1-2 (αK^d, *lane 4*). Likewise, lysate precipitated twice with 34-1-2 (*lanes 6* and *7*) and two times with protein A-Sepharose (not shown) was reacted with AP tail (*lane 8*). APLP2 recovered with AP tail or coprecipitated with the K^d-specific mAb 34-1-2 without prior treatment is shown in *lanes 1* and *5* or *lanes 6* and *9*, respectively. Quantitative analysis was carried out using a phosphor imager. The proportion of APLP2 not associated with K^d (*lane 8*) accounts for 35% (3900 relative units) of the total amount of APLP2 shown in *lanes 6–8* (11,600 relative units; protein A-precipitated material of rounds 3 and 4 was not considered). Control reactions in *lanes 1–4* reveal similar levels of APLP2 protein (14,400 relative units) as in *lanes 6–8*. Reagents used and the rounds of immunoprecipitation are indicated at the *top*.

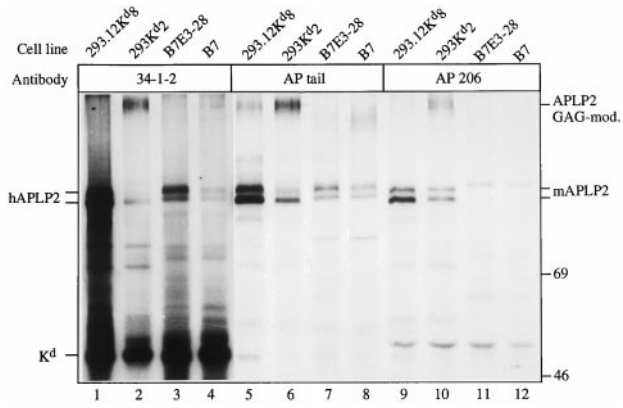

FIG. 5. **K^d also associates with murine APLP2 (*mAPLP2*).** K^d and APLP2 were immunoprecipitated from different cell lines radiolabeled for 1 h with 100 μCi/ml [^{35}S]methionine using mAb 34-1-2 against K^d and using AP tail and AP 206 directed to APLP2. The two human cell lines 293K^d2 and 293.12K^d8 were compared with murine SV40-transformed cell lines B7 and B7E3-28 expressing endogenous K^d in the absence or presence of E3/19K, respectively. Antiserum AP tail recognizes both human and murine APLP2 (*lanes 5–8*), whereas serum AP 206 specifically reacts with the human APLP2 protein (hAPLP2, *lanes 9–12*). The respective positions of murine and human APLP2 are indicated. Since B7E3–28 cells lack E1A, the expression level of E3/19K is only about 25% of that seen in 293.12K^d8 cells. Exposure time of *lanes 1–4* is 4-fold compared with that of *lanes 5–12*.

A Large Proportion of K^d Is Associated with APLP2—We next examined to what extent APLP2 is associated with K^d molecules in E3/19K^+ cells. Free K^d and APLP2-associated K^d molecules were depleted from radiolabeled lysates of 293.12K^d8 cells by successive rounds of immunoprecipitation with the K^d-specific monoclonal antibody 34-1-2 (αK^d). After two rounds of αK^d precipitation (Fig. 4, *lanes 6* and *7*) and two additional antibody-clearing steps using protein A-Sepharose (not shown), only about one-third of the total amount of APLP2 protein remains and can be precipitated by the AP tail antibody (compare *lane 8* with *lanes 1* and *5*). *Vice versa*, two successive rounds of immunoprecipitation with AP tail (Fig. 4, *lanes 1* and *2*) followed by two antibody-clearing steps (*lane 3*; second step not shown) and precipitation with αK^d (*lane 4*) shows that K^d is almost completely removed by APLP2 precipitation. Taken together, the results indicate that in E3/19K^+ cells a large proportion (about two-thirds) of the APLP2 protein is complexed with K^d molecules and that the great majority of K^d molecules is associated with APLP2.

K^d Also Associates with Murine APLP2—To investigate whether the murine MHC class I molecule K^d also associates with murine APLP2, K^d was immunoprecipitated from SV40-transformed fibroblast cell lines derived from BALB/c mice, either expressing (B7E3–28) or not expressing E3/19K (B7). Like in the equivalent human cell lines, 293K^d2 and 293.12K^d8, a small but significant amount of APLP2 is coprecipitated with K^d in the absence of E3/19K, and is strongly induced by coexpression of E3/19K (Fig. 5; compare *lanes 3* and *4* with *lanes 1* and *2*). The slightly reduced electrophoretic mobility of the two protein species coprecipitated in the murine cell lines is obviously a characteristic feature of murine APLP2, since the same differential mobility is also observed when APLP2 is directly precipitated using the AP tail serum (Fig. 5, compare *lanes 7* and *8* with *lanes 5* and *6*). Antiserum AP 206 does not recognize murine APLP2 (Fig. 5, *lanes 9–12*). In summary, binding to K^d is an intrinsic property of APLP2, and this activity is increased by the presence of E3/19K.

Remarkably, E3/19K expression appears to interfere with CS-GAG-modification of APLP2 in K^d-expressing cells as evidenced by the low amount of the CS-GAG-modified APLP2 form recovered in those cells (11% in 293.12K^d8 compared with 54% in 293K^d2 and 14% in B7E3–28 *versus* 36% in B7 cells during the labeling period). The altered processing of APLP2 is even more evident when the amount of CS-GAG-modified APLP2 coprecipitated with K^d is compared between E3/19K^+ and E3/19K^- cells. While in 293K^d2 cells 71% of the coprecipitated material is CS-GAG-modified, less than 5% is detected in 293.12K^d8 cells. Similar data were obtained for the murine cells (36% for B7 and 2% for B7E3–28). This indicates that the E3/19K-mediated inhibition of K^d transport also affects APLP2 transport, providing evidence that interaction occurs *in vivo*.

Coprecipitation of APLP2 with K^d Is Strictly Dependent on the Presence of β_2-Microglobulin and Is Increased by E3/19K—We next examined the structural requirements of K^d for APLP2 association and tested whether β_2m is necessary for this association. The human β_2m-negative cell line FO-1 (52) was transfected with K^d or both K^d and β_2m genes, resulting in cell lines constitutively expressing K^d and K^d/β_2m, respectively. Upon metabolic labeling and immunoprecipitation of K^d, proteins of similar molecular mass like APLP2 are specifically coprecipitated in K^d/β_2m-expressing cells (Fig. 6*A*, *lanes 5–8*). In contrast, no APLP2-like proteins are visualized in cells that express K^d in the absence of β_2m (Fig. 6*A*, *lanes 3* and *4*). Instead, another protein of ~90 kDa is detected that comigrates with the ER chaperone calnexin, known to interact with incompletely assembled MHC molecules (data not shown). To promote the interaction of APLP2 with K^d, we expressed E3/19K in these cells via infection with adenovirus type 2. Subsequently, K^d was immunoprecipitated using antibodies directed to various portions of K^d. Even after infection, no APLP2-specific proteins could be coprecipitated in lysates of β_2m^- cells (Fig. 6*B*, *FO-1K^d-4*, *lanes 1–4*) although they expressed E3/19K in similar amounts as β_2m^+ cells (Fig. 6*B*, compare *lanes 1* and *5*). Neither of the antibodies that recognized K^d in the absence of β_2m (antiserum Kc, directed to the cytoplasmic tail of K^d and detecting all K^d molecules, or mAb SF1–1.1.1, which recognizes the α3 domain of K^d) coprecipitated APLP2, whereas the same antibodies readily precipitated APLP2 from β_2m^+ cells (Fig. 6*B*, compare *lanes 6* and *7* with *lanes 2* and *3*). Interestingly, both antibodies coprecipitate the E3/19K protein, demonstrating that complex formation between MHC molecules and E3/19K does not require β_2m. MAb 34-1-2 directed to the α1/α2 domain of K^d is unable to react with K^d heavy chains even after

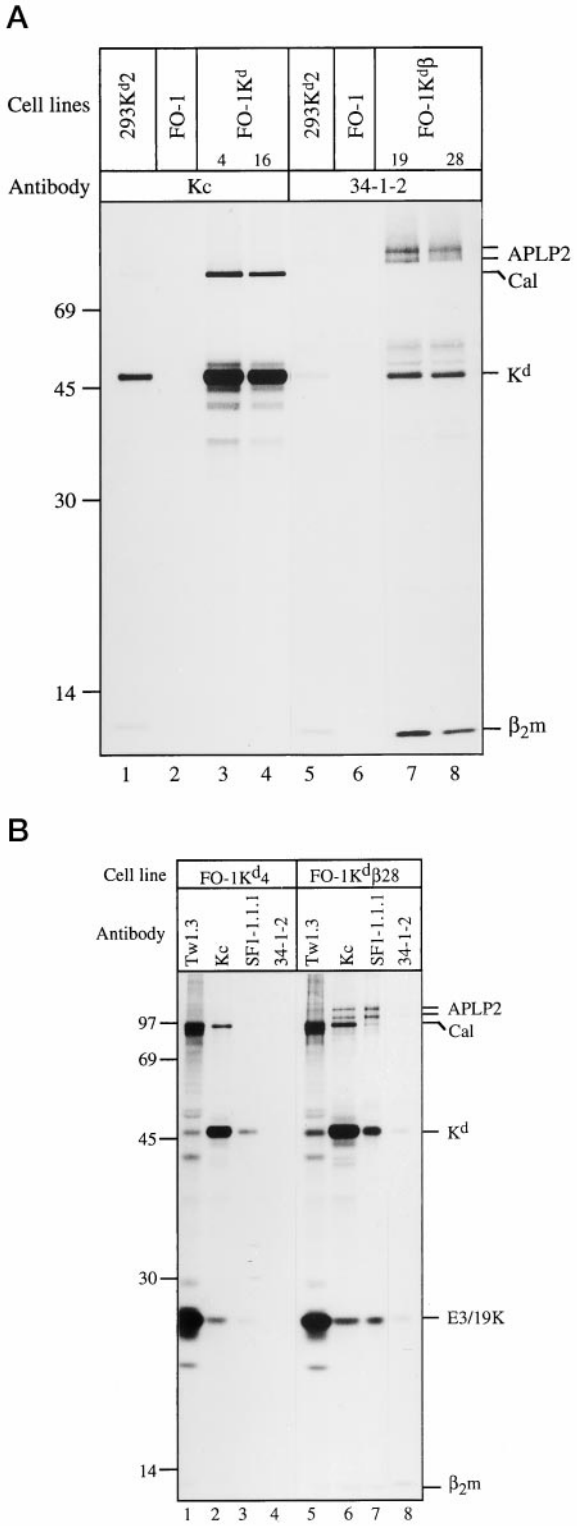

FIG. 6. **Binding of APLP2 to K^d requires β_2m.** *A*, expression of MHC K^d molecules in β_2m-negative and β_2m-positive FO-1 cells. The human melanoma cell line FO-1, which does not express β_2m, was transfected with K^d or both K^d and β_2m genes. The resulting cell lines were analyzed for K^d expression by immunoprecipitation with either Kc serum (FO-1K^{d}4 and FO-1K^{d}16) recognizing free K^d heavy chain (*lanes 1–4*) or with mAb 34-1-2 recognizing K^d/β_2m complexes (FO-1K$^d\beta$19 and FO-1K$^d\beta$28; *lanes 5–8*). Control immunoprecipitations were performed with 293K^{d}2 cells (*lanes 1* and *5*) and untransfected FO-1 cells (*lanes 2* and *6*). The positions of APLP2, calnexin (*Cal*), K^d heavy chain (*K^d*), and β_2m are indicated on the *right*; those of molecular weight markers are indicated on the left. *B*, E3/19K expression in β_2m-negative cells does not induce APLP2-K^d association. FO-1K^{d}4 and FO-1K$^d\beta$28 were infected with Ad2 for 15 h. After labeling with [^{35}S]methionine, lysates were reacted with antibodies directed to E3/19K (Tw1.3, *lanes 1* and *5*), the C terminus of K^d (Kc, *lanes 2* and *6*), the α3 domain (SF1–1.1.1, *lanes 3* and *7*), or the α1/α2 domain of K^d (34-1-2, *lanes 4* and *8*). The migration of the relevant proteins is indicated as in *A*.

the addition of K^d binding peptides (data not shown), indicating that this antibody requires β_2m for reactivity. Taken together, these data suggest that binding of E3/19K to MHC molecules occurs prior to the β_2m-HC association and that formation of the β_2m-K^d HC dimer is necessary for complex formation with APLP2.

Induction of K^d-APLP2 Association by E3/19K Requires Only the Cytoplasmic Portion of the E3/19K Molecule—The ability of the E3/19K molecule to promote complex formation between K^d and APLP2 may result from a conformational change of K^d induced by E3/19K binding. Alternatively, E3/19K mediated APLP2-K^d association may solely be due to the ability of E3/19K to retain K^d in the ER. To distinguish between these possibilities, a modified K^d protein was designed capable of staying in the ER. This was accomplished by replacing the cytoplasmic tail of K^d by that of E3/19K (Fig. 7*A*, K^{d}E3), thereby transferring the ER retrieval signal of E3/19K (KK*XX*; Ref. 41) to the K^d molecule. Indeed, the hybrid K^{d}E3 molecule cannot be detected on the cell surface of 293 cells stably expressing this construct (293K^{d}E3) as analyzed by fluorescence-activated cell sorting analysis (data not shown). Moreover, pulse-chase experiments did not reveal a significant transport of K^{d}E3 beyond the *cis*-Golgi (Ref. 54 and data not shown). To examine the ability of the mutant K^d protein to associate with APLP2, K^{d}E3 was immunoprecipitated from [^{35}S]methionine-labeled cells. For comparison, K^d molecules were also immunoprecipitated from cell lines expressing wild-type K^d in the absence (293K^{d}2) and presence of E3/19K (293.12K^{d}8; see the *schematic diagram* in Fig. 7*A*). As shown in Fig. 7*B*, the amount of coprecipitated APLP2 is drastically increased in K^{d}E3 immunoprecipitates compared with that seen when wild-type K^d molecules are immunoprecipitated from extracts of E3/19K-negative cells (Fig. 7*B*, compare *lanes 2* and *3*). Coprecipitation of APLP2 was as high as that observed when K^d molecules were extracted from E3/19K$^+$ cells (Fig. 7*B*, *lane 1*). The slightly faster mobility of K^{d}E3 is expected, since the cytoplasmic tail of the chimeric protein is shorter than that of the wild-type K^d molecule (15 instead of 40 aa). To rule out the possibility that the higher expression level of K^{d}E3 compared with that of K^d accounts for the higher amount of coprecipitating APLP2, transient transfections were performed using varying amounts of K^{d}E3 DNA. With 1.5 μg of K^{d}E3 DNA transfected, a comparable expression level of K^{d}E3 with that of K^d in 293.12K^{d}8 cells was achieved, and again a similar amount of coprecipitating APLP2 was observed (data not shown). These results demonstrate that the increased association of APLP2 with K^d does not require the physical presence of E3/19K but rather prolonged residency of K^d in the ER. However, the possibility of a direct influence of the cytoplasmic tail of E3/19K on K^d-APLP2 binding cannot be formally excluded.

Association of K^d with APLP2 Is Induced by Transport Inhibition—If ER retention of K^d is the major factor determining the extent of APLP2 association, other E3/19K-independent experimental conditions to inhibit transport of membrane proteins should also result in an increased APLP2 association. This was tested by employing BFA, a drug known to inhibit transport at the level of the Golgi by inducing retrograde Golgi-ER transport that leads to a redistribution of resident Golgi proteins into the ER (59). 293K^{d}2 and 293.12K^{d}8 cells were metabolically labeled in the absence or presence of BFA, and cell lysates were subjected to immunoprecipitation with

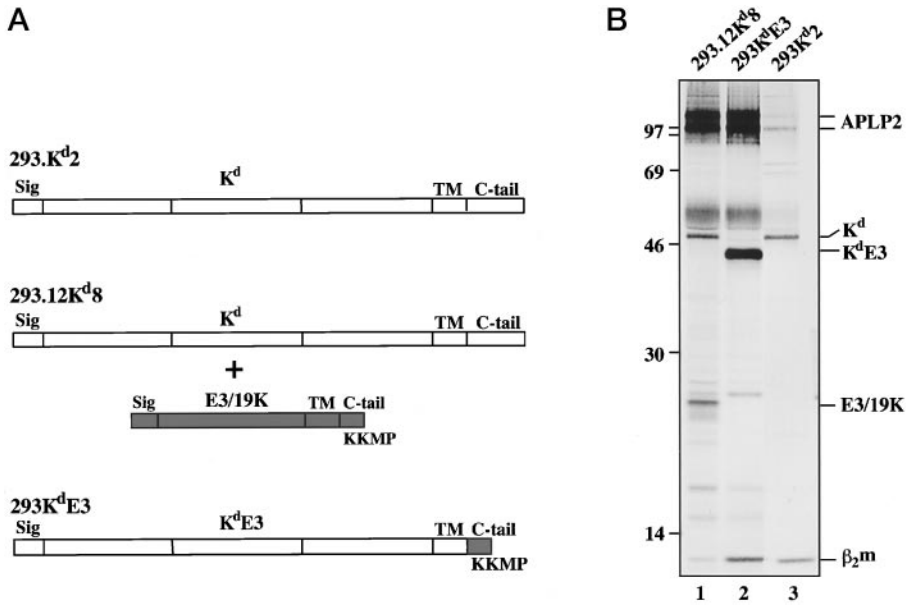

FIG. 7. **Association of APLP2 with K^d correlates with inhibition of K^d transport.** *A*, schematic representation of transfected genes in cell lines 293K^{d}2, 293.12K^{d}8, and 293K^{d}E3. *B*, cell lines indicated at the *top* were labeled with 100 μCi/ml [^{35}S]methionine, and equal amounts of radioactive lysates were precipitated using mAb 34-1-2. The positions of the respective proteins are indicated on the *right*.

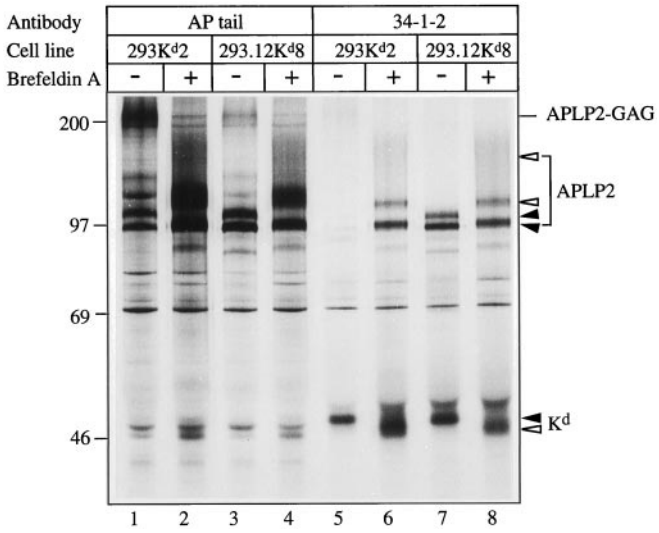

FIG. 8. **Transport inhibition by brefeldin A induces the association of APLP2 with K^d.** 293K^{d}2 and 293.12K^{d}8 cells were treated with 2.5 mg/ml brefeldin A, 3 h prior to and during the labeling period of 1 h (+). As controls, cells were mock-treated (−). Antiserum AP tail (*lanes 1–4*) and mAb 34-1-2 (*lanes 5–8*) were used to precipitate APLP2 and K^d, respectively.

antibodies 34-1-2 and AP tail (Fig. 8). In 293K^{d}2 cells, BFA treatment results in a profound increase (~8-fold) in the association of two proteins with K^d (Fig. 8, compare *lanes 5* and *6*). These coprecipitating proteins seem to represent APLP2 species, since comigrating proteins are detected when APLP2 is precipitated directly (Fig. 8, *lanes 2* and *4*) or coprecipitated by 34-1-2 in 293.12K^{d}8 cells (Fig. 8, *lane 8*). BFA treatment alters the mobility of the K^d and APLP2 proteins (*open arrowheads*), reflecting the modified carbohydrate side chains due to retrograde transport of various Golgi enzymes involved in carbohydrate processing. In contrast to 293K^{d}2 cells, BFA does not significantly increase the amount of coprecipitating APLP2 in 293.12K^{d}8 cells. The association of APLP2 with K^d was also induced when transport of membrane proteins was blocked by incubation of cells at 15 °C (data not shown). Taken together, these results demonstrate that conditions that inhibit the transport of K^d markedly increase its association with APLP2.

DISCUSSION

In this report, we have shown by several criteria that p100/110, the previously discovered high molecular weight proteins associated with the MHC K^d molecule in E3/19K$^+$ cells, are identical to APLP2. First, peptide sequences derived from purified p100/110 proteins were identical to those in APLP2 (Fig. 1). Second, three different antibodies raised against APLP2 precipitate proteins with the same apparent molecular mass as that of p100/110 and directly recognize p100/110 coprecipitated with K^d in Western blots and sequential immunoprecipitations (Figs. 2 and 3 and data not shown). Third, biochemical properties of p100/110 and APLP2, such as *N*-glycosylation and transmembrane orientation, are identical (Fig. 3, *A* and *B*). Moreover, we demonstrate that APLP2 binds K^d in the absence of E3/19K in human and mouse cells. Therefore, APLP2 exhibits an intrinsic affinity for the MHC K^d molecule. The adenovirus E3/19K protein profoundly increases complex formation between APLP2 and K^d due to its capacity to retain K^d in the ER. This was documented by the efficient association of APLP2 with the chimeric K^d/E3/19K molecule (K^{d}E3) that is targeted to the ER via the E3/19K tail. Corroborating the above results, we observed a reduced efficiency of APLP2-K^d interaction compared with E3/19K$^+$ cells if we coexpress E3/19K mutant molecules that lack either the ER retrieval signal or exhibit a decreased ability to interact with K^d (data not shown). Induction of APLP2-K^d association is also noted when the K^d and APLP2 molecules are retained by E3/19K-independent means. Thus, two conclusions can be drawn: (i) the physical presence of E3/19K is not essential for this interaction to occur, and (ii) conditions prolonging the transit of the K^d molecule through the ER/*cis*-Golgi enhance the proportion of K^d molecules that interact with APLP2.

Which of the four APLP2 isoforms (APLP2–763, -751, -707, or -695) interact with K^d molecules could not unequivocally be determined. In general, we only detect two primary protein species of 100–105 and 110–115 kDa, respectively. We previously showed that the different migration cannot be accounted for by differential *N*-linked glycosylation (Fig. 3*A*) or phosphorylation (30). Rather, the difference in apparent molecular mass of ~10 kDa suggests that these APLP2 species differ with regard to the presence of the KPI domain (calculated molecular mass: 6.6 kDa). Occasionally, each band was resolved as two species (data not shown), which may correspond to isoforms differing by the presence of the 12-aa peptide. Thus, the higher

molecular weight band (p110) seems to represent isoforms 763 and 751, and the lower molecular weight band (p100) seems to represent isoforms 707 and 695. In isoforms APLP2–751 and APLP2–695, which lack the 12-aa insert, the sequence SG*X*G is preceded by acidic amino acids, a requirement for GAG modification (60). Thus, only these forms are expected to undergo CS-GAG modification. Since K^d proteins were found in association with CS-GAG-modified and unmodified APLP2 (Fig. 5), we conclude that all four alternatively spliced APLP2 isoforms exhibit K^d binding activity. In agreement with this hypothesis, GAG modification is greatly impaired in the presence of E3/19K, indicating that APLP2 is retained in the ER via its interaction with K^d, whose transport is blocked by E3/19K (Fig. 5).

At present, we know little about the structural features necessary for this interaction to occur. Despite the sequence similarity and the homologous domain structure of APP and APLP2, we could not detect any association with APP, even after overexpression of APP (data not shown). Therefore, structural features of APLP2 distinct from APP must be responsible for binding to K^d. Candidate regions are the short stretch C-terminal to the KPI domain and the ~100 aa N-terminal to the putative membrane-spanning segment, including the Aβ domain, in which the APLP2 sequence is most divergent from that of APP (3–5, 11). With regard to the structure of K^d important for APLP2 binding, we show that *N*-linked carbohydrates are not essential for the interaction (Fig. 3*A*). However, we demonstrate that APLP2 association with K^d is strictly dependent on the presence of β_2m. APLP2 binding is not visible in β_2m^- cells, even in the presence of E3/19K. Since a direct interaction of APLP2 and β_2m could not be detected (data not shown), these data indicate that the association of APLP2 and K^d requires prior assembly of the class I HC/β_2m complex. Furthermore, folding of the α3 domain of K^d, which occurs in the absence of β_2m, as evidenced by the reactivity of mAb SF1–1.1.1, and suffices for binding to E3/19K, is not sufficient for APLP2 binding. By contrast, APLP2 association coincides with the acquisition of antibody epitopes present in the α1/α2 domains (*e.g.* that of 34-1-2; Ref. 30). Together, the data suggest that the conformational change within the α1/α2 domains accompanying or following β_2m binding is inducing APLP2 association. As previously proposed (30), APLP2 may be related to an as yet uncharacterized 105-kDa protein, whose coprecipitation with MHC D^b molecules is induced by an excess of human β_2m (61).

Previous data suggested a role of APLP2 during assembly or peptide loading of MHC I molecules. Several lines of evidence support this assumption. First, APLP2 and MHC I molecules exhibit an ubiquitous expression pattern and are both localized to the secretory compartment (3, 13, 18). Second, interaction with APLP2 only occurs in the presence of β_2m (Fig. 6). The same requirement exists for the association of empty class I molecules with TAP (18, 27, 62, 63). Third, reminiscent of the dissociation of completely folded MHC molecules from TAP upon peptide loading (19, 20), K^d-binding peptides trigger the displacement of APLP2 from the complex with K^d-β_2m/E3/19K (30). Thus, conditions essential for the interaction of class I molecules with TAP are also crucial for complex formation between K^d and APLP2. Intriguingly, E3/19K has been reported to bind to TAP (64). Together, these data support the idea that APLP2 plays a role in peptide transfer to K^d, *e.g.* in stabilization of empty α1/α2 domains. Alternatively, APLP2 may bind during the peptide transfer step to MHC K^d molecules, assisting its final folding or regulating by its KPI activity a putative peptide trimming protease and escorting the complex to the cell surface. This latter hypothesis is based on the known inhibition of various proteases by the KPI domains of APP and APLP2 (65) and the interaction of K^d with GAG-modified APLP2, which implies that complexes exist beyond the ER. Whether complexes are present on the cell surface and, if so, whether these complexes serve a specific function remains to be investigated.

Interestingly, we routinely observe a prominent protein species of ~51–57 kDa coprecipitating with the K^d-E3/19K-APLP2 complex (Figs. 3*B* and 7; Ref. 30), which may be identical or related to the recently identified MHC I-associated ER-resident chaperone ERp57 with thiol-reductase activity (19, 20, 23, 66). It has been proposed that this protein may be involved in oxidation of MHC I molecules or in trimming longer TAP translocated peptides. Both suggestions are compatible with its putative APLP2/K^d association. It is also possible that the coprecipitated protein of ~55 kDa is related to p60 that binds peptides in the lumen of the ER (31).

While a strong interaction of APLP2 was only observed with K^d, weak interactions with HLA could be detected using more sensitive assays, such as immunoprecipitation of digitonin lysates combined with Western blotting (data not shown). At present, we do not know which feature of the K^d molecule makes it more sensitive to complex formation with APLP2 than other MHC alleles. Transport of the K^d molecule is rather slow, which may allow prolonged interaction. However, no Nonidet P-40 stable APLP2 complexes are detected with other MHC molecules having a similar export rate such as L^d, D^b, and HLA-C (data not shown). Interestingly, allelic differences exist for the association of MHC molecules with TAP and their dependence from tapasin for peptide loading (27, 28). For example, HLA-B*2705 can be efficiently loaded with peptide in the absence of tapasin, while loading of HLA-B8 or HLA-B*4402 molecules is profoundly impaired under these conditions. Thus, differential requirements for the interaction of MHC alleles with proteins involved in MHC assembly and peptide loading do exist; therefore, differential requirements may also exist for complex formation of MHC molecules with APLP2.

The interaction of APLP2 with the MHC K^d molecule described above is a novel activity of the APLP2 protein. Based on the structural similarity of APLP2 with APP, similar suggestions have been made as to the functions of both molecules, including a function as cell surface receptor (1, 67, 68), as adhesion molecule involved in axogenesis (69), as a growth factor for the secreted ectodomain (70), or as a DNA-binding protein with a role in DNA segregation during early embryonic development (5, 10). Recently, it was realized that many antibodies raised against APP cross-react with APLP2 and *vice versa* (13). Thus, a number of previous studies are difficult to interpret, since APP and APLP2 are not discriminated. In addition, the widely different functions suggested for APLP2 may be explained in part by the different systems employed, the number of isoforms present in the cells, and the difference in developmental stage (embryonic *versus* adult).

One hypothesis previously put forward suggests that APLP2 acts as cell surface receptor. In line with such a proposal, we observe complexes of K^d with CS-GAG-modified APLP2 in E3/19K-negative cells (Fig. 5), demonstrating that complexes do exist beyond the ER in the medial/trans-Golgi, where CS-GAG modification takes place, and possibly on the cell surface. To our knowledge, this is the first example of an APP family member forming physical complexes with immunologically relevant molecules. There are precedents for interactions between MHC molecules and other proteins seemingly unrelated to their antigen presentation function. For example, tetraspanin molecules like CD82 form complexes with MHC I molecules

(71). In addition, the murine cytomegalovirus protein gp34 has been shown to escort MHC molecules to the cell surface (72). In both cases, it was speculated that these MHC I-binding proteins may modulate cytotoxic T cell or natural killer cell recognition. Determination of whether APLP2 influences the function of K^d on the cell surface requires further investigation.

Our studies reveal a novel, surprising mechanism for downregulation of APLP2 from the cell surface. By expression of E3/19K, which retains K^d in the ER, the expression of an unrelated molecule, APLP2, is also affected. This mechanism is operating in the murine system, since we could show an interaction of K^d with murine APLP2. Therefore, it is tempting to speculate that other (murine) viruses that target the antigen presentation pathway and retain class I molecules in the ER, such as murine cytomegalovirus (51), could also interfere with transport of APLP2. The functional consequences of an impaired cell surface expression await further clarification.

Acknowledgments—We are grateful to S. Ferrone, H. Hengel, J. Bennink, K. Beyreuther, and V. Herzog for the gifts of cells, plasmids, and antibodies. We thank C. Ebenau-Jehle and A. Osterlehner for excellent technical assistance. For critical reading of the manuscript we thank Z. Ruzsics, R. Baumeister, and D. Schendel.

REFERENCES

1. Selkoe, D. J. (1998) *Trends Cell Biol.* **8,** 447–453
2. Wasco, W., Bupp, K., Magendantz, M., Gusella, J. F., Tanzi, R. E., and Solomon, F. (1992) *Proc. Natl. Acad. Sci. U. S. A.* **89,** 10758–10762
3. Wasco, W., Gurubhagavatula, S., d. Paradis, M., Romano, D. M., Sisodia, S. S., Hyman, B. T., Neve, R. L., and Tanzi, R. E. (1993) *Nat. Genet.* **5,** 95–100
4. Sprecher, C. A., Grant, F. J., Grimm, G., O'Hara, P. J., Norris, F., Norris, K., and Foster, D. C. (1993) *Biochemistry* **32,** 4481–4486
5. von der Kammer, H., Hanes, J., Klaudiny, J., and Scheit, K. H. (1994) *DNA Cell Biol.* **13,** 1137–1143
6. Rosen, D. R., Martin-Morris, L., Luo, L. Q., and White, K. (1989) *Proc. Natl. Acad. Sci. U. S. A.* **86,** 2478–2482
7. Daigle, I., and Li, C. (1993) *Proc. Natl. Acad. Sci. U. S. A.* **90,** 12045–12049
8. Zheng, H., Jiang, M. H., Trumbauer, M. E., Sirinathsinghji, D. J. S., Hopkins, R., Smith, D. W., Heavens, R. P., Dawson, G. R., Boyce, S., Conner, M. W., Stevens, K. A., Slunt, H. H., Sisodia, S. S., Chen, H. Y., and van der Ploeg, L. H. T. (1995) *Cell* **81,** 525–531
9. von Koch, C. S., Zheng, H., Chen, H., Trumbauer, M., Thinakaran, G., van der Ploeg, L. H., Price, D. L., and Sisodia, S. S. (1997) *Neurobiol. Aging* **18,** 661–669
10. Rassoulzadegan, M., Yang, Y., and Cuzin, F. (1998) *EMBO J.* **17,** 4647–4656
11. Sandbrink, R., Masters, C. L., and Beyreuther, K. (1994) *J. Biol. Chem.* **269,** 14227–14234
12. Bush, A. I., Pettingell, W. J., de Paradis, M., Tanzi, R. E., and Wasco, W. (1994) *J. Biol. Chem.* **269,** 26618–26621
13. Slunt, H. H., Thinakaran, G., Von Koch, C., Lo, A. C. Y., Tanzi, R. E., and Sisodia, S. S. (1994) *J. Biol. Chem.* **269,** 2637–2644
14. Pangalos, M. N., Shioi, J., and Robakis, N. K. (1995) *J. Neurochem.* **65,** 762–769
15. Thinakaran, G., Slunt, H. H., and Sisodia, S. S. (1995) *J. Biol. Chem.* **270,** 16522–16525
16. Lo, A. C. Y., Thinakaran, G., Slunt, H. H., and Sisodia, S. S. (1995) *J. Biol. Chem.* **270,** 12641–12645
17. Townsend, A., and Bodmer, H. (1989) *Annu. Rev. Immunol.* **7,** 601–624
18. Pamer, E., and Cresswell, P. (1998) *Annu. Rev. Immunol.* **16,** 323–358
19. Lehner, P. J., and Trowsdale, J. (1998) *Curr. Biol.* **8,** 605–608
20. van Endert, P. M. (1999) *Curr. Opin. Immunol.* **11,** 82–88
21. Hammond, C., and Helenius, A. (1995) *Curr. Opin. Cell Biol.* **7,** 523–529
22. Sadasivan, B., Lehner, P. J., Ortmann, B., Spies, T., and Cresswell, P. (1996) *Immunity* **5,** 103–114
23. Lindquist, J. A., Jensen, O. N., Mann, M., and Hämmerling, G. J. (1998) *EMBO J.* **17,** 2186–2195
24. Koopmann, J. O., Hämmerling, G. J., and Momburg, F. (1997) *Curr. Opin. Immunol.* **9,** 80–88
25. Grandea, A. G., Androlewicz, M. J., Athwal, R. S., Geraghty, D. E., and Spies, T. (1995) *Science* **270,** 105–108
26. Ortmann, B., Copeman, J., Lehner, P. J., Sadasivan, B., Herberg, J. A., Grandea, A. G., Riddell, S. R., Tampé, R., Spies, T., Trowsdale, J., and Cresswell, P. (1997) *Science* **277,** 1306–1309
27. Neisig, A., Wubbolts, R., Zang, X. S., Melief, C., and Neefjes, J. J. (1996) *J. Immunol.* **156,** 3196–3206
28. Peh, C. A., Burrows, S. R., Barnden, M., Khanna, R., Cresswell, P., Moss, D. J., and McCluskey, J. (1998) *Immunity* **8,** 531–542
29. Srivastava, P. K., and Udono, H. (1994) *Curr. Opin. Immunol.* **6,** 728–732
30. Feuerbach, D., and Burgert, H.-G. (1993) *EMBO J.* **12,** 3153–3161
31. Marusina, K., Reid, G., Gabathuler, R., Jefferies, W., and Monaco, J. J. (1997) *Biochemistry* **36,** 856–863
32. Solheim, J. C., Harris, M. R., Kindle, C. S., and Hansen, T. H. (1997) *J. Immunol.* **158,** 2236–2241
33. Burgert, H.-G. (1996) *Trends Microbiol.* **4,** 107–112
34. Hengel, H., and Koszinowski, U. H. (1997) *Curr. Opin. Immunol.* **9,** 470–476
35. Früh, K., Ahn, K., and Peterson, P. A. (1997) *J. Mol. Med.* **75,** 18–27
36. Burgert, H.-G., and Kvist, S. (1985) *Cell* **41,** 987–997
37. Andersson, M., Paäbo, S., Nilsson, T., and Peterson, P. A. (1985) *Cell* **43,** 215–222
38. Burgert, H.-G., Maryanski, J. L., and Kvist, S. (1987) *Proc. Natl. Acad. Sci. U. S. A.* **84,** 1356–1360
39. Flomenberg, P., Piaskowski, V., Truitt, R. L., and Casper, J. T. (1996) *J. Virol.* **70,** 6314–6322
40. Gabathuler, R., and Kvist, S. (1990) *J. Cell Biol.* **111,** 1803–1810
41. Jackson, M. R., Nilsson, T., and Peterson, P. A. (1990) *EMBO J.* **9,** 3153–3162
42. Cox, J. H., Bennink, J. R., and Yewdell, J. W. (1991) *J. Exp. Med.* **174,** 1629–1637
43. Jackson, M. R., Nilsson, T., and Peterson, P. A. (1993) *J. Cell Biol.* **121,** 317–333
44. Cosson, P., and Letourneur, F. (1994) *Science* **263,** 1629–1631
45. Pääbo, S., Weber, F., Nilsson, T., Schaffner, W., and Peterson, P. A. (1986) *EMBO J.* **5,** 1921–1927
46. Burgert, H.-G., and Kvist, S. (1987) *EMBO J.* **6,** 2019–2026
47. Sester, M., and Burgert, H.-G. (1994) *J. Virol.* **68,** 5423–5432
48. Feuerbach, D., Etteldorf, S., Ebenau-Jehle, C., Abastado, J. P., Madden, D., and Burgert, H.-G. (1994) *J. Immunol.* **153,** 1626–1636
49. Deryckere, F., and Burgert, H.-G. (1996) *J. Virol.* **70,** 2832–2841
50. Körner, H., Fritzsche, U., and Burgert, H.-G. (1992) *Proc. Natl. Acad. Sci. U. S. A.* **89,** 11857–11861
51. Del Val, M., Hengel, H., Hacker, H., Hartlaub, U., Ruppert, T., Lucin, P., and Koszinowski, U. H. (1992) *J. Exp. Med.* **176,** 729–738
52. D'Urso, C. M., Wang, Z. G., Cao, Y., Tatake, R., Zeff, R. A., and Ferrone, S. (1991) *J. Clin. Invest.* **87,** 284–292
53. Weidemann, A., König, G., Bunke, D., Fischer, P., Salbaum, J. M., Masters, C. L., and Beyreuther, K. (1989) *Cell* **57,** 115–126
54. Lapham, C. K., Bacik, I., Yewdell, J. W., Kane, K. P., and Bennink, J. R. (1993) *J. Exp. Med.* **177,** 1633–1641
55. Andersson, S., Davis, D. L., Dahlback, H., Jornvall, H., and Russell, D. W. (1989) *J. Biol. Chem.* **264,** 8222–8229
56. Popp, G. M., Graebert, K. S., Pietrzik, C. U., Rosentreter, S. M., Lemansky, P., and Herzog, V. (1996) *Endocrinology* **137,** 1975–1983
57. Elsing, A., and Burgert, H.-G. (1998) *Proc. Natl. Acad. Sci. U. S. A.* **95,** 10072–10077
58. Gavel, Y., and von Heijne, G. (1990) *Protein Eng.* **3,** 433–442
59. Lippincott-Schwartz, J., Donaldson, J. G., Schweizer, A., Berger, E. G., Hauri, H. P., Yuan, L. C., and Klausner, R. D. (1990) *Cell* **60,** 821–836
60. Esko, J. D., and Zhang, L. (1996) *Curr. Opin. Struct. Biol.* **6,** 663–670
61. Townsend, A., Elliott, T., Cerundolo, V., Foster, L., Barber, B., and Tse, A. (1990) *Cell* **62,** 285–295
62. Carreno, B. M., Solheim, J. C., Harris, M., Stroynowski, I., Connolly, J. M., and Hansen, T. H. (1995) *J. Immunol.* **155,** 4726–4753
63. Suh, W. K., Cohen-Doyle, M. F., Früh, K., Wang, K., Peterson, P. A., and Williams, D. B. (1994) *Science* **264,** 1322–1326
64. Bennett, E. M., Bennink, J. R., Yewdell, J. W., and Brodsky, F. M. (1999) *J. Immunol.* **162,** 5049–5052
65. Van Nostrand, W. E., Schmaier, A. H., Neiditch, B. R., Siegel, R. S., Raschke, W. C., Sisodia, S. S., and Wagner, S. L. (1994) *Biochim. Biophys. Acta* **1209,** 165–170
66. Oliver, J. D., van der Wal, F. J., Bulleid, N. J., and High, S. (1997) *Science* **275,** 86–88
67. Nishimoto, I., Okamoto, T., Matsuura, Y., Takahashi, S., Okamoto, T., Murayama, Y., and Ogata, E. (1993) *Nature* **362,** 75–79
68. Kang, J., Lemaire, H. G., Unterbeck, A., Salbaum, J. M., Masters, C. L., Grzeschik, K. H., Multhaup, G., Beyreuther, K., and Muller-Hill, B. (1987) *Nature* **325,** 733–736
69. Thinakaran, G., Kitt, C. A., Roskams, A. J., Slunt, H. H., Masliah, E., von Koch, C., Ginsberg, S. D., Ronnett, G. V., Reed, R. R., Price, D. L., and Sisodia, S. S. (1995) *J. Neurosci.* **15,** 6314–6326
70. Saitoh, T., Sundsmo, M., Rock, J.-M., Kimura, N., Cole, G., Schubert, D., Oltersdorf, T., and Schenk, D. B. (1989) *Cell* **58,** 615–622
71. Lagaudriere-Gesbert, C., Lebel Binay, S., Wiertz, E., Ploegh, H. L., Fradelizi, D., and Conjeaud, H. (1997) *J. Immunol.* **158,** 2790–2797
72. Kleijnen, M. F., Huppa, J. B., Lucin, P., Mukherjee, S., Farrell, H., Campbell, A. E., Koszinowski, U. H., Hill, A. B., and Ploegh, H. L. (1997) *EMBO J.* **16,** 685–694